175. Formation and Structure of the Phosphoranyl Radical Derived from 1,2-Phenylene Phosphorochloridate: a Solid-State ESR Study

by **Maria Cattani-Lorente, Gérald Bernardinelli,** and **Michel Geoffroy***

Department of Physical Chemistry and Laboratory of Crystallography, 30, quai Ernest Ansermet, CH-1211 Geneva 4

(27.VII.87)

The crystal structure of 1,2-phenylene phosphorochloridate has been determined. X-Ray irradiation of these crystals, at low temperature, leads to the formation of a radical exhibiting hyperfine structure with P and Cl nuclei. The corresponding ESR tensors are obtained, and they show that this radical is a phosphoranyl radical adopting a slightly distorded σ^* structure. The same species could be produced in frozen solution, its hyperfine tensors are, then, more in accordance with a trigonal-bipyramid structure. The effects of the host matrix on the stabilization of the structure of phosphoranyl are investigated.

1. Introduction. – In the past ten years, there has been a considerable interest in the structure of phosphoranyl radicals [1]. While the first experimental investigations had shown that these species generally adopt a trigonal-bipyramid structure with the unpaired electron located in the equatorial position (TBP-e) [2][3], our ESR study [4] of $Ph_3\dot{P}Cl$ led to a trigonal pyramid with the unpaired electron in a σ^* orbital. Several additional structures have also been proposed: the trigonal bipyramid with the unpaired electron in axial position (TBP-a) [5] and the distorded σ^* structure [6][7].

The most suitable method for the study of radical's structures is obviously the single-crystal ESR technique, particularly, when the ESR tensors can be related to the crystal structure of the undamaged molecule. However, the participation of the crystal

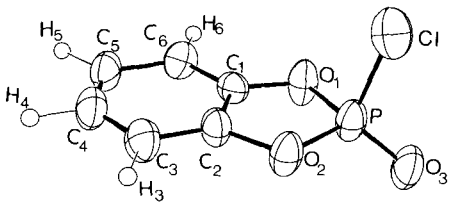

1

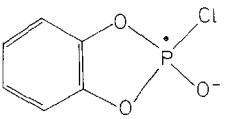

2

lattice in the stabilization of the observed structure cannot be totally excluded, particularly with such a finely-balanced system as the phosphoranyl radical. In the present study, we have determined the crystal structure of the phosphorochloridate compound **1**, and we tried to trap, in the crystal matrix, the phosphoranyl radical **2** resulting from the electron capture by the P=O bond.

To know, if the crystal matrix is involved in the stabilization of the observed structure, we have attempted to produce the same phosphoranyl radical **2** in frozen solutions for detecting the subsequent structure modifications.

2. Experimental. – 1,2-phenylene phosphorochloridate *(Aldrich)* is a moisture-sensitive and corrosive compound (m.p. 55°). Large single crystals were obtained by slowly cooling a quartz tube containing the molten compound. The tube was then broken at r.t. under Ar, and a single-crystal fragment was rapidly glued on a small brass cube which was slowly immersed in liquid N_2. The crystal was irradiated at 77 K for 2 h (X-ray *Philips* tube with a W anticathode, 30 mA, 30 kV). The X-irradiated crystal was mounted in a finger *Dewar* containing liquid N_2 and oriented in the magnet of the ESR spectrometer *(Bruker 200D*, X-band, 100-kHz field modulation). The undefined morphology of the crystal together with the experimental difficulties (low melting point and instability of the crystal) compelled us to use an arbitrary ESR reference frame. The temp. dependence of the ESR spectra was investigated by using a *Bruker VT 1100* temp. controller. Photolysis experiments were performed by exposing the sample, directly in the ESR cavity, to the focused radiation of a high-pressure Hg vapor lamp. The simulation of the ESR spectra obtained with the polyoriented samples were obtained by using a second-order perturbation program which sums the spectra calculated for 120000 random orientations of the magnetic field. These calculations take the g-tensor and the ^{31}P and the ^{35}Cl magnetic hyperfine interactions into account.

The crystal used for the X-ray structure determination was obtained by zone melting in a *Lindemann* capillary of 0.5 mm. Monoclinic; space group *I2*; $a = 7.889(4)$, $b = 9.115(2)$, $c = 10.469(2)$ Å; $\beta = 95.37(2)°$; $Z = 4$; $D_c = 1.688$ gcm^{-3}; $\mu = 6.66$ cm^{-1}. The lattice parameters and intensities were measured at r.t. on a automatic four-circle *Philips PW1100* diffractometer with a graphite monochromator using MoK_α radiation ($\lambda = 0.71069$ Å) and refined by full matrix least-squares. The structure was solved by direct methods (Multan 80 [8]) and refined by full-matrix least-squares. Atomic scattering factors and anomalous dispersion terms for Cl-, P-, and O-atoms from International Tables for X-Ray Crystallography [9]. All coordinates of H-atoms were calculated. The final R factor, based on the 1217 observed reflections ($|F_o| \geq 4\sigma(F_o)$ and $|F_o| \geq 8$) was 0.041. All calculations performed with a local version of XRAY76 [10] and ORTEPII [11].

The *ab-initio* calculations were performed by using the *Gaussian* 82 program [12]. The optimized geometry for $(OH)_3\hat{P}Cl$ was obtained from UHF calculations (4-31G* basis set) by using gradient optimizations techniques [13].

3. Results. – *Crystal Structure*[1]). Positional parameters and equivalent isotropic temperature factors are given in *Table 1*. Bond distances and relevant bond angles are given in *Table 2*. The O(1), P,O(2) plane makes an angle of 7.4° with the benzene ring. The P-atom is located in the *ac* plane; this plane is practically the bisector plane of the O(1), P,O(2) angle and also contains the P–Cl and P–O(3) bonds.

Table 1. *Fractional Coordinates and Equivalent Isotropic Temperature Factors* U_{eq} [Å^2 × 10^3] (e.s.d.'s in parentheses; U_{eq} is the average of the eigenvalues of U)

	x	y	z	U_{eq}
Cl	0.89608(11)	0	0.30042(10)	70.3(4)
P	0.67719(11)	− 0.0013(6)	0.37977(8)	49.3(3)
O(1)	0.5713(10)	− 0.1373(7)	0.3084(6)	52.4(18)
O(2)	0.5728(11)	0.1272(7)	0.3171(5)	51.5(20)
O(3)	0.7040(3)	− 0.0057(12)	0.51820(21)	65.0(9)
C(1)	0.4561(13)	− 0.0784(10)	0.2171(8)	37.7(22)
C(2)	0.4506(13)	0.0730(10)	0.2163(8)	43.7(23)
C(3)	0.3461(14)	0.1556(14)	0.1326(8)	51(4)
C(4)	0.2471(14)	0.0773(13)	0.0489(9)	53(3)
C(5)	0.2339(14)	− 0.0744(13)	0.0422(9)	53(3)
C(6)	0.3500(12)	− 0.1556(11)	0.1323(7)	45(3)

[1]) Crystallographic data has been deposited with the *Cambridge Crystallographic Data Center*, University Chemical Laboratory, Lensfield Road, Cambridge CB2 1EW, England.

Table 2. *Interatomic Distances* [Å] *and Relevant Bond Angles* [°] (e.s.d.'s in parentheses)

Cl–P	1.985(2)	C(1)–C(2)	1.381(12)
P–O(1)	1.636(8)	C(1)–C(6)	1.358(12)
P–O(2)	1.543(8)	C(2)–C(3)	1.371(14)
P–O(3)	1.445(3)	C(3)–C(4)	1.326(15)
O(1)–C(1)	1.366(11)	C(4)–C(5)	1.389(17)
O(2)–C(2)	1.449(11)	C(5)–C(6)	1.455(14)
Cl–P–O(1)	103.9(3)	O(2)–P–O(3)	118.0(5)
Cl–P–O(2)	105.6(3)	P–O(1)–C(1)	107.5(6)
Cl–P–O(3)	111.6(1)	P–O(2)–C(2)	110.1(6)
O(1)–P–O(2)	98.7(4)	O(1)–C(1)–C(2)	114.5(8)
O(1)–P–O(3)	117.2(5)	O(2)–C(2)–C(1)	108.5(7)

Electron Spin Resonance. a) *Single Crystal.* An example of an ESR spectrum obtained at 77 K with an X-irradiated single crystal of $C_6H_4O_3PCl$ is shown in *Fig. 1*; two sets of lateral signals, marked A, are clearly observed besides a broad central line. The angular

Table 3. *Experimental ESR Tensors Obtained with Irradiated 1,2-Phenylene Phosphorochloridate*

Single Crystal Measurements		Direction cosines		
Radical A				
g-tensor	$g_1 = 2.0036$	− 0.833	− 0.380	0.401
	$g_2 = 2.0071$	0.040	0.682	0.730
	$g_3 = 2.0080$	0.551	− 0.624	0.553
^{31}P-T (MHz)	$T_1 = 2924$	− 0.159	0.718	− 0.678
	$T_2 = 3017$	0.012	0.688	0.726
	$T_3 = 3230$	0.987	0.108	− 0.118
^{35}Cl-T (MHz)	$T_1 = 86$	− 0.375	0.680	− 0.629
	$T_2 = 118$	0.023	0.685	0.728
	$T_3 = 189$	− 0.926	− 0.259	0.273
Radical B				
g-tensor	$g_1 = 2.002$	$g_{min}(A)$, $g_{min}(B) = 59°$		
	$g_2 = 2.005$			
	$g_3 = 2.008$			
^{31}P-T (MHz)	$T_1 = 2938$			
	$T_2 = 2983$			
	$T_3 = 3262$	^{31}P-$T_{max}(A)$, ^{31}P-$T_{max}(B) = 49°$		
^{35}Cl-T (MHz)	$T_1 = 78$			
	$T_2 = 84$			
	$T_3 = 182$	^{35}Cl-$T_{max}(A)$, ^{35}Cl-$T_{max}(B) = 45°$		
Radical in Frozen Solution[a])				
g-tensor	$g_1 = 1.999$	0.940	− 0.342	0
	$g_2 = 2.004$	0.342	0.940	0
	$g_3 = 2.008$	0	0	1
^{31}P-T (MHz)	$T_1 = 3140$	1	0	0
	$T_2 = 2781$	0	1	0
	$T_3 = 2800$	0	0	1
^{35}Cl-T (MHz)	$T_1 = 105$	0.985	− 0.174	0
	$T_2 = 185$	0.174	0.985	0
	$T_3 = 80$	0	0	1

[a]) The principal axes of the ^{31}P-hyperfine tensor are arbitrarily used as reference axes.

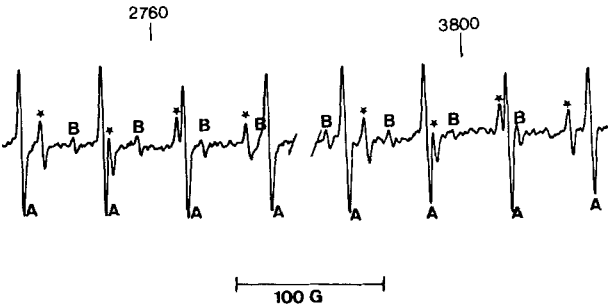

Fig. 1. *ESR spectrum obtained at 77 K from an X-irradiated single crystal of $C_5H_4O_3PCl$ previously annealed at 155 K.* Signals marked B are not observed before annealing. Signals due to radical A are marked A(^{35}Cl) and * (^{37}Cl).

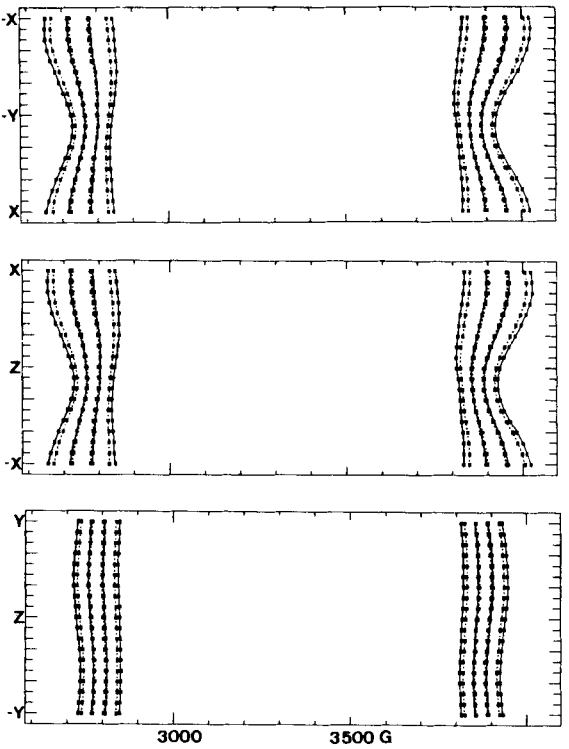

Fig. 2. *Angular dependence of signals A*

dependance of the signals A is shown in *Fig. 2*. It is clear that this pattern is due to a radical-exhibiting hyperfine structure with a ^{31}P nucleus (natural abundance 100%, I = 1/2) and with a ^{35}Cl nucleus (natural abundance 75%, I = 3/2). For almost all orientations, the signals due to ^{37}Cl are also detected. The g and hyperfine tensors obtained by using a second-order perturbation and an optimization program are given in *Table 3*. The forbidden transitions ($\Delta M_I = \pm 1$) for the chlorine nuclei are observed for some orientations, they are expected to be sensitive to the quadrupolar interaction Q, but

their angular variation led us to estimate Q as being inferior to 9 MHz. This interaction is weak and the lack of precision due to the line width (Γ = 6 G) precludes any structural interpretation of this coupling.

When the crystal is slightly heated to 155 K, additional weak signals, marked B, appear in the region of the A lines. The appearance of these signals B has been detected with all the investigated crystals. Their angular dependance has been studied on a crystal previously used for the determination of the tensors of radical A. Both a phosphorus and a chlorine nucleus participate to the hyperfine structure of radical B. The corresponding data are given in *Table 3*.

b) *Polyoriented Samples.* The ESR spectrum obtained at 77 K with an X-irradiated polycrystalline sample of **1** is shown in *Fig. 3* together with the ESR spectrum simulated by using the tensors obtained for radical A from single-crystal measurements. The ESR spectra obtained with X-irradiated frozen solutions of **1** are quite different from the powder spectrum. Besides a central part, probably due to irradiated solvant molecules, the spectra obtained with Et_2O or THF exhibit lateral signals which are characteristic of hyperfine interaction with ^{31}P and ^{35}Cl nuclei (*Fig. 4*). These signals are obviously due to a phosphoranyl radical, but the simulation of the corresponding spectrum is not straightforward. Indeed, the various tensors are not axial, and their principal axes are not aligned; the best simulation we could obtain is shown in *Fig. 4* and the corresponding tensors are given in *Table 3*.

Photolysis at 77 K of the polycrystalline X-irradiated sample leads to a rapid decay of the phosphoranyl radical; a similar behaviour is observed with the frozen solutions, but, in this latter case, the disappearance of the lateral spectrum is accompanied by the

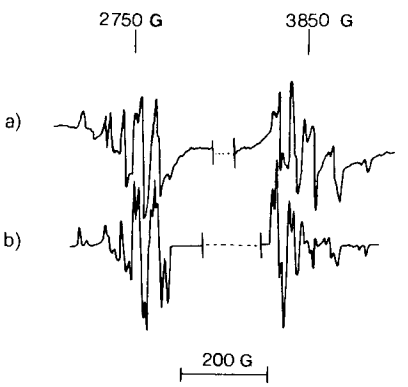

Fig. 3. a) *ESR spectrum obtained at 77 K with X-irradiated polycrystalline sample of* **1**. b) *Powder spectrum simulated by using the ESR tensors obtained from the single-crystal study* (radical A, *Table 3*).

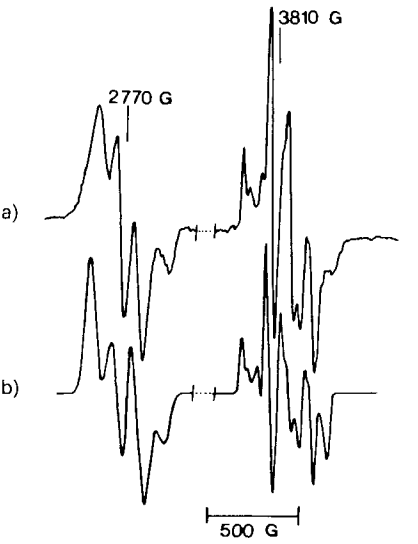

Fig. 4. a) *ESR spectrum obtained at 77 K from an X-irradiated frozen solution of* **1** *in* Et_2O. b) *Simulated spectrum obtained by using the tensors given in* Table 3 (frozen solution).

formation of a new phosphorus-centered radical (radical C). The appearance of this secondary species was not observed, when the frozen solution had not been irradiated prior to photolysis.

Calculations. To get a theoretical indication about the most stable structure of a $(RO)_2P(Cl)OR'$ radical, we have calculated by *ab-initio* methods the optimized structure of $(HO)_2\dot{P}(Cl)OH$. Since the presence of the five-membered ring imposes an O(1),P,O(2) angle close to 100° for **1**, we have first attempted to optimize the structure of $(HO)_2\dot{P}(Cl)OH$ by keeping this angle constant. Unfortunately, under these conditions, no convergence could be obtained. We have, then, imposed the P–Cl bond to be located on a C_3 axis. The optimized structure (E = 1025.5053 a.u.) is given in *Table 4*. The corresponding expectation value $< S^2 >$ is equal to 0.758 and the calculated spin densities are listed in *Table 4*.

Table 4. *Optimized Geometry and Calculated Spin Densities for $(HO)_3PCl$ (ab-initio* calculations)

Bond distance [Å]	P–Cl =	2.074	P–O =	1.622	O–H =	0.952		
Bond angle [°]	∢ OPCl =	90.36	∢ OPO =	119.99	∢ POH =	111.23		
Torsion angle [°]	ClPOH	179.98						
Spin densities	ρ [P(3s)] =	0.23	ρ [P($3p_x$)] =	−0.02	ρ [(P($3p_y$)] =	−0.02	ρ [P($3p_z$)] =	0.48
	ρ [Cl(3s)] =	0.00	ρ [Cl($3p_x$)] =	0.00	ρ [Cl($3p_y$)] =	0.00	ρ [Cl($3p_z$)] =	0.00
	ρ [0_1(3s)] =	0.00	ρ [0_1($3p_x$)] =	0.08	ρ [0_1($3p_y$)] =	0.00	ρ [0_1($3p_z$)] =	0.02

4. Discussion. – The hyperfine tensors obtained for radical A lead to the isotropic and anisotropic coupling constants shown in *Table 5*. The ^{31}P-isotropic constant clearly shows that the species A is a phosphoranyl radical, and the presence of the chlorine hyperfine structure is totally consistent with the trapping of **2**.

Although the presence of two sites can be forseen from the crystal symmetry, only one site is observed for all the orientations. Taking into account the fact that the six eigenvectors g_1, g_3, $^{31}P-T_1$, $^{31}P-T_3$, $^{35}Cl-T_1$, and $^{35}Cl-T_3$ are coplanar *(Table 2)*, the existence of a single site implies that the common direction g_2, $^{31}P-T_2$, $^{35}Cl-T_2$ is aligned along the *b* axis. As shown by the crystal structure, the *ac* plane is parallel to the symmetry plane of the molecule, the g_1, g_3, $^{31}P-T_3$, $^{31}P-T_1$, $^{35}Cl-T_1$, and $^{35}Cl-T_3$ directions, therefore, belong to the bissector plane of the O(1), P,O(2) angle of the undamaged molecule.

Table 5. *Isotropic and Anisotropic Coupling Constants and Corresponding Spin Densities Obtained by Using the Atomic Parameters Given in* [14]

Radical	A_{iso} [MHz]		τ_{aniso} [MHz][a])		Spin densities[a])		Angle ($^{31}P-T_{max}$, $^{35}Cl-T_{max}$)
	^{31}P	^{35}Cl	^{31}P	^{35}Cl	P	Cl	
A	3057	131	− 133	− 45 (− 81)	$c_s^2 = 0.23$	$c_s^2 = 0.02$ (0.00)	12°
			− 40	− 13 (− 113)	$c_p^2 = 0.24$	$c_p^2 = 0.16$ (0.55)	
			173	58 (194)			
B	3061	115	− 123	− 37 (− 85)	$c_s^2 = 0.23$	$c_s^2 = 0.02$ (0.00)	17.5°
			− 78	− 31 (− 91)	$c_p^2 = 0.27$	$c_p^2 = 0.19$ (0.50)	
			201	68 (176)			
In frozen solution	2097	123	233	− 18 (− 105)	$c_s^2 = 0.16$	$c_s^2 = 0.02$ (0.00)	80°
			− 126	62 (185)	$c_p^2 = 0.31$	$c_p^2 = 0.18$ (0.52)	
			− 107	− 44 (− 80)			

[a]) The values in parentheses are calculated by taking $T_\parallel > 0$ and $T_\perp < 0$.

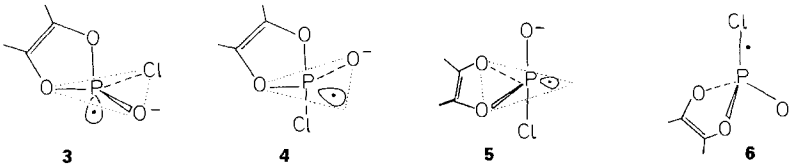

3 4 5 6

An additional point to be noted is the small value of the angles formed by the g_{max}, $^{31}P-T_{max}$, and $^{35}Cl-T_{max}$ directions ($\sphericalangle\ ^{31}P-T_{max}$, $^{35}Cl-T_{max} = 12°$). These angular properties allow us to eliminate several structures: the TBP-a **3** and the TBP-e **4** (the $^{31}P-T_{max}$ eigenvector would not lie in the O(1), P,O(2) bissector), and the TBP-e **5** (the angle $\sphericalangle\ ^{31}P-T_{max}$, $^{35}Cl-T_{max}$ would be close to 90°). The single acceptable structure is the C_s structure **6** in which the unpaired electron is located in the P–Cl σ^* orbital: the $^{35}Cl-T_{max}$ and the $^{31}P-T_{max}$ directions are almost aligned, and they lie in the *ac* plane. In fact, this geometry does not need any drastic modification of the undamaged molecule, and it can be easily obtained by a slight deplacement of the O(3)- and Cl-atoms inside the molecular symmetry plane. The phosphorus and chlorine spin densities, calculated by using the atomic-coupling constants published by *Morton* and *Preston* [14], are shown in *Table 5*. They are similar to the values reported for other phosphoranyl radicals.

The formation of radical B is a more puzzling problem. There is no doubt that the spin densities found for this radical *(Table 5)* can be assigned to a phosphoranyl radical with a structure very similar to that found for A. The main difference between A and B resides in the two distinct orientations of the eigenvectors (*e.g.* $\sphericalangle\ ^{35}Cl-T_{max}(A)$, $^{35}Cl-T_{max}(B) = 50°$). The radical B is not directly produced by irradiation, but it seems to result from a thermal conversion of radical A. The experimental information is, however, insufficient to give a description of this process (radical reorientation, phase transition ...), nevertheless this temperature dependance suggests that the crystal matrix may have some effect on the ESR tensors of the phosphoranyl radical.

The ESR spectra recorded with the polyoriented samples clearly indicate that the tensors found for radical **1** in a crystalline matrix are no longer valid in frozen solution. The values reported in *Table 3* show that, in a frozen solution, the $^{31}P-T_{max}$ direction makes an angle of 70° with the $^{35}Cl-T_{max}$ direction. This property is in accord with a slightly distorted TBP-e structure **4** and contrasts sharply with the structure **6** found in the crystal. The effect of the environment is also apparent in the light decomposition process of the phosphoranyl radical. The radical C, produced in small amount during photolysis of **1** in frozen solution, is characterized by a ^{31}P splitting of $\sim$ 730 G and does not exhibit any ^{35}Cl hyperfine interaction. This species, which is probably the phosphonyl radical **7**, could never been observed in the crystalline matrix. However, we cannot exclude a reaction in which radicals formed from solvent molecules would be involved.

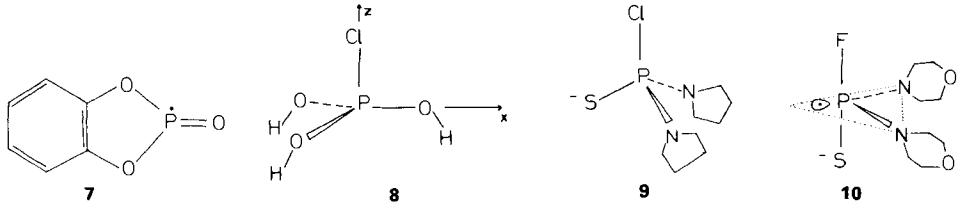

7 8 9 10

Table 6. *Structural Parameters for Some Phosphoranyl Radicals*

Radical	Spin densities		Angle	Ref.
	P	Cl	$\sphericalangle$ (^{31}P–T_{max}, ^{35}Cl–T_{max})	
$Ph_3\dot{P}Cl$	$c_s^2 = 0.13$	0.01	7°	[4]
	$c_p^2 = 0.44$	0.25		
9	$c_s^2 = 0.19$	0.01	29°	[7]
	$c_p^2 = 0.44$	0.13		
10	$c_s^2 = 0.17$	0.02	82°	[7]
	$c_p^2 = 0.32$	0.13		

The optimized structure calculated for $(HO)_3\dot{P}Cl$ *(Table 4)* is close to a trigonal pyramid with the Cl-atom located on the ternary axis. However, the large O,P,O angle is incompatible with the presence of the ring in radical **2**. The difference between the experimental results and the theoretical structure **8** clearly appears in the chlorine spin densities $\rho_{exp}(Cl) = 20\%$, $\rho_{theor.}(Cl) = 0\%$. Unfortunately, fixing a reasonable value for one of the three O,P,O angles prevented us getting any optimized structure. Such a problem of convergence has already been reported by *Janssen et al.* [7] for $(NH_2)_2\dot{P}(Cl)S^-$ and $(NH_2)_2\dot{P}(F)S^-$, although these authors could trap the radicals **9** and **10** in crystalline samples *(Table 6)*.

It is, therefore, probable that interactions between phosphoranyl radical and the surrounding molecules play a decisive role in the stabilization and the reactivity of these radicals. This is in accord with the great variety of phosphoranyl structures found in the literature and with the present study which shows that the shape of radical **2** is a distorted trigonal pyramid in a crystal matrix, but changes toward a trigonal bipyramid in frozen solution.

Financial support of these investigations by the *Swiss National Science Foundation* is gratefully acknowledged.

REFERENCES

[1] For a review on the structure and formation of phosphoranyl: W. G. Bentrude, *Acc. Chem. Res.* **1982**, *15*, 117; R. A. J. Janssen, Ph. D. thesis, Unversity of Eindhoven, 1987.
[2] T. Gillbro, F. Williams, *J. Am. Chem. Soc.* **1974**, *96*, 5132.
[3] A. Hasegawa, K. Ohnishi, K. Sogabe, M. Miura, *Mol. Phys.* **1975**, *36*, 677.
[4] T. Berclaz, M. Geoffroy, E. A. C. Lucken, *Chem. Phys. Lett.* **1975**, *36*, 677.
[5] J. H. H. Hammerlinck, P. Schipper, P. Buck, *J. Am. Chem. Soc.* **1980**, *102*, 5679.
[6] M. Geoffroy, A. Llinares, E. Krzywanska, *J. Magn. Reson.* **1984**, *58*, 389.
[7] R. A. J. Janssen, M. H. W. Sonnemans, H. M. Buck, *J. Am. Chem. Soc.* **1986**, *108*, 6145.
[8] P. Main, S. J. Fiske, S. E. Hull, L. Lessinger, G. Germain, J. P. Declercq, M. M. Woolfson, 1980, A system of computer Programs for the Automatic Solution of Crystal Structures from X-Ray Diffraction Data. Universities of York, England, and Louvain- La-Neuve, Belgium.
[9] International Tables for X-Ray Crystallography, 1974, Vol. IV, Birmingham, Kynoch Press.
[10] J. M. Stewart, P. A. Machin, C. W. Dickinson, H. L. Ammon, H. Heck, H. Flack, 1976, The Xray'76 System. Tech. Rep. TR446. Computer Science Center, Univ. of Maryland, College Park, Maryland.
[11] C. K. Johnson, 1976, ORTEP II. Report ORNL-5138. Oak Ridge National Laboratory, Tennessee.
[12] a) J. S. Binkley, R. A. Whiteside, R. Krishnan, R. Seeger, D. J. De Frees, H. B. Schlegel, S. Topiol, L. R. Kahn, J. A. Pople. *Q.C.P.E.* **1981**, *13*, 406; b) J. S. Binkley, M. J. Frisch, D. J. De Frees, K. Raghavachari, R. A. Whiteside, H. B. Schlegel, E. M. Fluder, J. A. Pople. GAUSSIAN 82, Carnegie-Mellon University, Pittsburg, 1983.
[13] J. S. Binkley, *J. Chem. Phys.* **1976**, *64*, 5143; R. Fletcher, M. J. D. Powell, *Compt. J.* **1973**, *6*, 163.
[14] J. R. Morton, K. F. Preston, *J. Magn. Reson.* **1978**, *30*, 577.